sustainability

MDPI

Article

An Electric Vehicle Charging Method Considering Multiple Power Exchange Modes' Coordination

Long Zeng [1], Si-Zhe Chen [1,*], Zebin Tang [1], Ling Tian [2] and Tingting Xiong [3]

[1] School of Automation, Guangdong University of Technology, Guangzhou 510006, China; zenglong2404@gdut.edu.cn (L.Z.); t-zb@163.com (Z.T.)
[2] Electric Power Research Institute of China Southern Power Grid, Guangzhou 510663, China; tianling@csg.cn
[3] China Southern Power Grid Guangdong Zhuhai Power Supply Company, Zhuhai 519000, China; xiongtingting@zh.gd.csg.cn
* Correspondence: sizhe.chen@gdut.edu.cn

Abstract: To achieve sustainable environmental development, numerous countries and governments have been vigorously promoting the proliferation of electric vehicles (EVs) through a series of policy measures and economic subsidies. With the increasing number of EVs, multiple EV charging modes are being researched to satisfy owners' requirements. In this paper, an EV charging method considering multiple power exchange modes' coordination is proposed for meeting owners' requirements with cost-effectiveness. In the proposed method, the battery swapping (BS) station, building-to-vehicle (B2V) station, and grid-to-vehicle (G2V) station are considered. In G2V stations, EVs charge from the power grid. In B2V stations, distributed renewable energy generation is considered as the energy provider. This study contemplates the use of photovoltaic power systems in B2V stations for the charging of EVs. In BS stations, the power exchange among batteries and the power grid is considered. The battery energy storage is utilized for reducing the battery degradation cost (BDC) and power cost. EVs are dispatched to the corresponding charging stations according to the electric price, BDC, and so on. In the dispatching process, the particle swarm optimization (PSO) algorithm and Hungarian algorithm are applied. Several case studies are presented to validate the effectiveness of the proposed method and the power matching between EVs and charging modes is discussed.

Keywords: electric vehicle; charging mode; user's requirement; vehicle-to-grid; battery swapping

Citation: Zeng, L.; Chen, S.-Z.; Tang, Z.; Tian, L.; Xiong, T. An Electric Vehicle Charging Method Considering Multiple Power Exchange Modes' Coordination. *Sustainability* **2023**, *15*, 10520. https://doi.org/10.3390/su151310520

Academic Editors: Hengrui Ma, Xiaoying Wang, Yujuan Fang and Yanbo Chen

Received: 1 June 2023
Revised: 22 June 2023
Accepted: 2 July 2023
Published: 4 July 2023

1. Introduction

The transportation sector is considered as one of the largest of the sectors that pollute the environment [1], especially in countries that have achieved success in integrating environmentally friendly energies into the energy mix, such as China. To address pollution issues induced by vehicular exhaust emissions, electric vehicles (EVs) powered by clean energy may well serve as an effective and foreseeable means to achieve low-carbon sustainable development. Numerous countries and governments, driven by their commitments to sustainable development and environmental protection targets, have implemented a range of incentive policies that facilitate the rapid growth of EVs. Moreover, due to their eco-friendly characteristics and lower costs compared to fossil fuel-powered alternatives, EVs have received tremendous attention.

The number of EVs has increased considerably in recent years [2]. With the increasing number of EVs, the owners' requirements have become diverse and complex [3]. In different scenarios such as commercial and residential, EV owners' requirements present unique characteristics and should be satisfied through the corresponding charging mode [4].

To satisfy EV owners' requirements, various charging modes were proposed and applied. In the charging modes, the EV charging load is coordinated according to the distributed renewable energy generation, electricity price, and users' constraints. Grid-to-vehicle (G2V) is a smart charging technology that allows bi-directional power flow between

EVs and the power grid [5–9]. In [10], EV charging power was adjusted according to the initial state-of-charge (SOC), real-time SOC, object SOC, and plug-in period. This method met EV owners' driving requirements and mitigated the adverse impact of EV charging on the power grid. In [11,12], the control center guided EV charging and discharging during the load valley and load peak periods, respectively. In the guiding process, information such as electricity price was fluctuating and collected by the control center. The battery degradation cost (BDC) is increased with the frequent charging and discharging of EVs' batteries. In [13], EVs as flexible resources participated in the electricity market ancillary services. The quick and accurate power adjusting maintained the normal operation of the power system effectively. G2V is a common charging mode to satisfy owners' driving requirements, and the mode is constrained by the charging space and the regular system signals such as the load curve and electricity price.

Building-to-vehicle (B2V) and home-to-vehicle (H2V) charging modes are extensions of the G2V mode. B2V and H2V are both smart charging technology that allows bi-directional power flow between EV batteries and microgrids. In the microgrids, flexible loads and renewable power generation (RPG) are considered [14–20]. The increasing EVs are integrated into the RPG systems to overcome power and environmental limitations. EVs are essential for reducing greenhouse gas emissions through consuming the RPG [21]. This integration is particularly beneficial in residential power distribution, where EVs can provide an ancillary service [22]. EV charging load and other flexible loads are coordinated to concentrate on the low electricity price period or the surplus RPG period. In [23,24], EVs were considered as the flexible load that consumed RPG locally and considered as the energy providers that discharge power to the load in the microgrid. The power cost of the home microgrid and building microgrid was decreased by utilizing the EV's power storage capacity. In [25,26], the energy management system adjusted the EV's charging power with the real-time electricity price and the household load. This model may not fully meet the quick energy replenishment requirement of EV users. In [27–29], the EV's charging scheme in the microgrids was optimized for online operation. During the charging process, the load and resources in the microgrids are coordinated for local consumption of RPG and low power cost. B2V and H2V are constrained by the electric price, load, and RPG curves in the microgrid.

Considering the disadvantages of G2V, H2V, and B2V modes such as charging space constraints, charging time, or cost constraints, battery swapping (BS) mode is considered as an efficient charging mode and is applied for solving EV charging queue and parking problems. In [30], a two-stage energy management method was proposed. During the first stage, the BS scheme was optimized for satisfying users' driving requirements, and the battery charging scheme in the BS station was optimized in the second stage for reducing the power cost. When a large number of EVs drive to a BS station, the total cost will be increased significantly. In [31], the real-time electricity price was considered and batteries in the station were charged during the cheap price period. In [32–35], a BS station was considered as a battery aggregator in an area and significantly improved the local consumption of RPG. In [36–38], BS and G2V modes were coordinated satisfied EV users' requirements and maintained the normal operation of the power grid. A BS station with lots of batteries is considered as a flexible resource with sufficient capacity. It plays an obvious role in the local consumption of RPG and in maintaining the normal operation of the power system.

The existing EV charging modes could meet the users' driving requirements. However, it is difficult to satisfy users' driving requirements with cost-effectiveness. This is because each charging mode with unique characteristics just meets some users' requirements in certain scenes. In this paper, an EV charging method considering BS, B2V, and G2V modes is proposed. In the proposed method, the multiple charging modes are coordinated to meet users' driving and economic requirements. In the G2V mode, the cost of charging EVs can be reduced by utilizing the electricity price difference. In B2V mode, the RPG is considered as an energy provider in microgrids and guided EV charging load. In BS mode, the power

exchange among batteries and the power grid is considered in the optimization process. In each period, EVs are dispatched to the corresponding power exchange mode to reduce the power cost and BDC.

In the dispatching process, the particle swarm optimization (PSO) algorithm and Hungarian algorithm are applied. PSO is a population-based optimization algorithm that does not rely on gradient information [39]. It has a solid global search capability but may converge more slowly around the local optimum. In this paper, the number of EVs that are dispatched to stations is considered as the decision variable, which is an array. To improve the convergence speed, the Hungarian algorithm is applied for obtaining the optimal EV dispatching scheme for each PSO particle.

The remainder of this paper is organized as follows. In Section 2, the EV charging modes' coordination method is presented. In Section 3, numerous case studies are shown and discussed deeply. Finally, conclusions are drawn in Section 4.

2. Methodology

2.1. System Framework

In Figure 1, the EV charging system includes charging EVs, a G2V station, a B2V station, and a BS station. The EV charging process is hierarchical to reduce the cost. At the lower level, the charging system collects information such as the user's requirement, electricity price, the number of charging EVs, RPG, and so on. According to the collected information, EVs are dispatched to the corresponding charging stations. At the upper level, the power exchange in each charging station is optimized considering the unique characteristics.

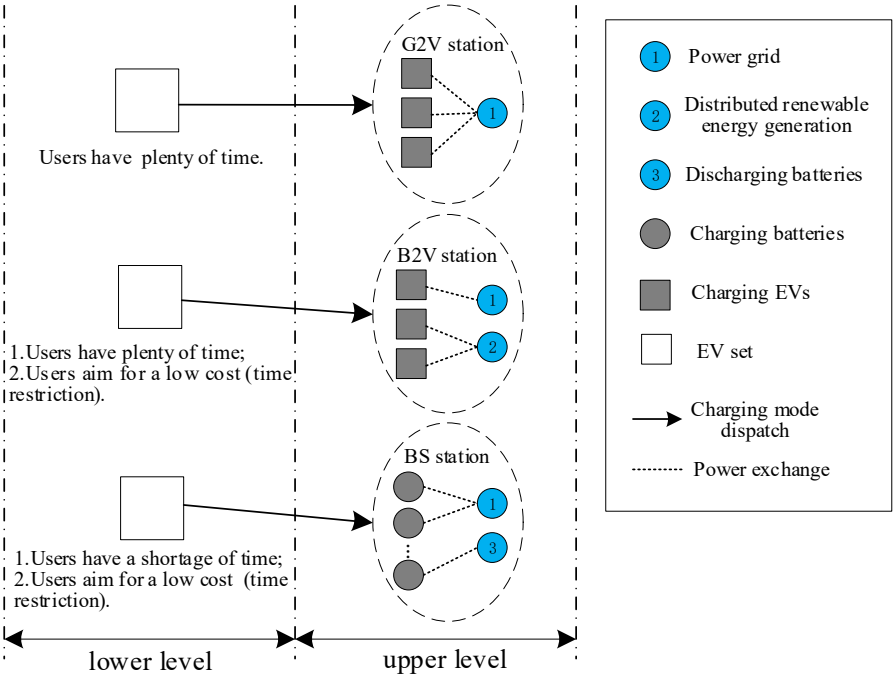

Figure 1. Framework of EV charging system.

In the G2V station, the electricity price is changing and affects the total cost of EV users. In the B2V station, the RPG is considered. RPG and the electricity price are both important factors that affect the user's cost. In the BS station, the B2B charging mode is considered during the high electricity price period and the battery charging load is concentrated in the low electricity price period. G2V charging will generate a low cost if the electricity price of the charging period is cheap. B2V charging may generate a low cost when RPG is abundant. EVs supplement energy by BS mode and may generate a low cost when the idle batteries are sufficient. In the BS station, the batteries could charge from the power grid

and other batteries according to the electricity price. When the electricity price is exorbitant, the batteries in the BS station may charge from other batteries to reduce the power cost. Every charging mode has a unique characteristic and is suitable for certain kinds of users.

2.2. Problem Formulation

2.2.1. G2V Charging Station

In the G2V station, EV charging power in each period is scheduled. The charging scheme is affected by the EV parking period and real-time price.

$$C_n(t) = (P_n(t) \cdot \Delta t) \cdot a_{Grid}(t) + BDC_n(t), \tag{1}$$

$$SOC_n(t_{end}) = SOC_n(t_{ini}) + \frac{\int_{t_{ini}}^{t_{end}} P_n(t)dt}{Q_n}, \tag{2}$$

$$BDC_n(t) = C_{pur}\left(\beta(\frac{P_n(t)}{Q_n} + 1 - SOC_n(t))^{\gamma} - \beta(1 - SOC_n(t))^{\gamma}\right), \tag{3}$$

$$\begin{cases} SOC_{\min} \le SOC_n(t) \le SOC_{\max} \\ SOC_n(t_{end}) \ge SOC_{n,obj} \end{cases}, \tag{4}$$

$$P_{\min} \le P_n(t) \le P_{\max}, \tag{5}$$

where C_n is the cost of the nth EV, and the unit is \$. The cost includes the power cost and battery degradation cost. P_n is the charging power of the nth EV, and the unit is kW. Δt is the time interval, and the unit is h. $a_{Grid}(t)$ is the electricity price of the power grid at t period, the unit is \$/kWh. BDC_n is the battery degradation cost of the nth EV, and the unit is \$. SOC_n is the SOC of the nth EV's battery. t_{ini} and t_{end} are the initial and end time of the EV plug in the power grid, respectively, and the units are h. Q_n is the rated capacity of the nth EV's battery, and the unit is kWh. C_{pur} is the acquisition cost of an EV battery, the unit is \$. β and γ are the model parameters. $SOC_{n,obj}$ is the object SOC of the nth EV's battery. $SOC_{\max}$ and $SOC_{\min}$ are the maximum and minimum SOC values of the EV battery, respectively. $P_{\min}$ and $P_{\max}$ are the minimum and maximum charging power of the EV battery, respectively, and the units are kW.

In (1), EV charging cost includes the power cost and BDC during the charging process. The power cost varies depending on the charging power and real-time electricity price. The BDC varies depending on the charging power and the SOC value of the battery as shown in (3) [13]. It shows that the SOC of the battery can be considered as a constant value during Δt. In (2), the SOC value of the EV battery is changing with the charging power at each parking period, and the real-time SOC value is constrained in a rational range as shown in (4). It prevents battery over-charging and over-discharging. The final SOC value of the EV battery is no less than the object SOC value for ensuring the user's driving requirement. When the EV's battery reaches the object SOC value, the charger will cease charging the battery. In (5), the charging power is constrained in a rational range. In this paper, the charging power is more than zero that means the battery charges from resources. The charging power is no more than zero that means the battery discharges to other batteries.

2.2.2. B2V Charging Station

H2V and B2V are considered as similar charging modes in different scenarios. In this paper, B2V is considered in the subsequent theoretical analysis and simulations. In the B2V

station, RPG in the microgrid is considered to reduce EV power cost. The output power and electricity price both affect the power cost.

$$\sum_{n=1}^{N_{B2V}} P_n(t) + P_{B,load}(t) - P_{B,RPG}(t) - P_{Grid}(t) = 0, \tag{6}$$

$$\begin{cases} C_n(t) = P_n^*(t) \cdot a_{Grid}(t) + BDC_n(t), \; if \; P_n^*(t) > 0 \\ C_n(t) = BDC_n(t), \quad or \; else \end{cases}, \tag{7}$$

$$P_n^*(t) = \sum_{n=1}^{N_{B2V}} P_n(t) + (P_{B,load}(t) - P_{B,RPG}(t)), \tag{8}$$

$$\begin{cases} SOC_{\min} \le SOC_n(t) \le SOC_{\max} \\ SOC_n(t_{end}) \ge SOC_{n,obj} \end{cases}, \tag{9}$$

$$P_{\min} \le P_n(t) \le P_{\max}, \tag{10}$$

where N_{B2V} is the number of EVs dispatched to the B2V station. $P_{B,load}$ is the total load in the microgrid, kW. $P_{B,RPG}$ is the output power of RPG in the microgrid, kW. P_{Grid} is the power purchasing from or selling to the power grid, kW. P_n^* is the power that EV charges from the power grid, kW.

In (6), the EV charging load is coordinated to maintain the balance between supply and demand in the microgrid. In this process, EVs are considered as flexible resources with fast response speed, and the power grid is considered as the energy prosumer with considerable capacity. Therefore, in the B2V charging station, EVs could charge from RPG and the power grid. The power cost in B2V mode will be no more than that in G2V mode as shown in (7). In (8), the output power of RPG is priority consumed by the power load and then consumed by EV charging load. In (9) and (10), the constraints protect EV batteries by preventing battery over-charging and over-discharging. Similar to (5), the charging power is limited by the maximum charging power and the minimum charging power which is no more than zero.

2.2.3. BS Station

In the BS station, EVs can supplement energy in a short time. The real-time electricity price affects the power cost, and the power cost in BS mode will be no more than the other two modes due to adequate preparation time. Due to this reason, the BDC in BS mode will also be no more than the other two modes.

$$C_{BSS}(t) = P_{BS}(t) \cdot a_{Grid}(t) + \sum_{b=1}^{N_{BS}} BDC_b(t), \tag{11}$$

$$C_n = \sum_{t'=t_0}^{t} P_b(t') \cdot a_{Grid}(t') + \sum_{t'=t_0}^{t} BDC_b(t'), \tag{12}$$

$$P_{BS}(t) = \sum_{b=1}^{N_{BS}} P_b(t), \tag{13}$$

$$P_b(t) = P_{Grid}(t) + \sum_{b'=1}^{N_{BS}-1} P_{b'}(t), \tag{14}$$

$$C_{BDC,b} = \sum_{t'=t_0}^{t} BDC_b(t') + 2 \cdot \sum_{b'} \sum_{t'=t_0}^{t} BDC_{b'}(t'), \sum_{t'=t_0}^{t} P_{b'}(t') \ne 0, \tag{15}$$

$$\begin{cases} SOC_{b\min} \le SOC_b(t) \le SOC_{b\max} \\ SOC_b(t_{end}) \ge SOC_{n,obj} \end{cases}, \tag{16}$$

$$P_{b\min} \le P_b(t) \le P_{b\max}, P_{b\min} \le 0, \tag{17}$$

where C_{BSS} is the cost resulting from battery charging, \$. The cost includes the power cost and BDC. P_{BS} is the total charging power provided by the power grid, kW. N_{BS} is the number of batteries in the BS station. $P_b(t')$ is the charging power of the bth battery in the previous period, kW. t_0 is the initial charging time of the battery, h. $SOC_{b\min}$ and $SOC_{b\max}$ are the minimum and maximum SOC values of batteries, respectively. $P_{b\max}$ and $P_{b\min}$ are the maximum and minimum charging power of the battery, respectively, kW. $P_{b'}$ is the B2B power, kW.

In (11), the total cost of the BS station includes the power cost and BDC. The former varies depending on the charging power and real-time electricity price. The latter varies depending on the SOC value of batteries and the charging power. The cost of swapping an EV battery depends on the power cost and BDC as shown in (12). Unlike G2V and B2V modes, the power cost and BDC could be reduced by adjusting the charging scheme in the idle period. Considering the load perk period with prohibitive electricity price, B2B mode is considered in the BS station. Some batteries charge from other batteries to satisfy users' requirements with a low power cost as shown in (14). However, the B2B mode will generate additional BDC due to the discharging process as shown in (15). In (16) and (17), the constraints protect the BS station's batteries to prevent battery over-charging and over-discharging. Similar to (5) and (10), the charging power of batteries is limited by the maximum and minimum charging power. Due to the B2B charging mode, the minimum charging power of batteries is less than zero.

2.3. Hierarchical Power Exchange Algorithm

2.3.1. Optimization Model

At lower power exchange, EVs are dispatched to G2V, B2V, and BS stations. In this process, the number of EVs that drive to each charging station is considered as the decision variable. The optimization result will have an impact on the optimization process at the upper power exchange.

$$\min \sum_{n=1}^{N_{EV}(t)} C_n(t), \tag{18}$$

s.t. (1)–(17)

$$\begin{cases} SOC_{b\min} < SOC_{n,obj}(t) \le SOC_{b\max} \\ SOC_{\min} < SOC_{n,obj}(t) \le SOC_{\max} \end{cases}, \tag{19}$$

$$\begin{cases} t_n = t_{n,end} - t_{n,ini} \\ t_n \ge t_{BS} \ge \frac{\left(SOC_{n,obj}(t_{n,end}) - SOC(t_{n,ini})\right) \cdot Q_n}{P_{\max}} \end{cases}, \tag{20}$$

where $N_{EV}(t)$ is the number of EVs dispatched to stations. $t_{n,end}$ and $t_{n,ini}$ are the end time and initial time of the nth EV's parking time, respectively, h. t_n is the nth EV's parking period, h. t_{BS} is the battery charging period in the BS station, h.

EV charging at a low cost could improve the user experience. Considering the number of charging EVs is random, the optimization object is the minimum cost of users at each period as shown in (18). In (19), the object SOC value of the EV battery is constrained within the normal range. EV parking period is defined and constrained as shown in (20). The constraint condition ensures the EV user's driving requirements can be satisfied.

2.3.2. Assumptions, Limitations, and Uncertainties

The following assumptions are raised in this research to facilitate the analysis:

- The maximum, minimum, and object SOC values for EVs are assumed to be constants.
- The random number of EVs starts at the 9th hour and ends at the 19th hour.

- EV parking duration at G2V and B2V stations is 2 h.

2.3.3. Optimization Method

At the lower level, EVs are dispatched to stations based on the particle swarm optimization algorithm and Hungarian algorithm to improve the convergence speed. At the upper level, the power exchange in G2V, B2V, and BS stations is optimized based on the particle swarm optimization algorithm. In the optimization process, the particle swarm optimization algorithm and the Hungarian algorithm are applied at lower power exchange to improve the convergence speed [40–42]. In this process, the number of EVs that are dispatched to charging stations is considered as the decision variable which is an array. Hungarian algorithm is used to obtain the optimal EV dispatching scheme for each particle of PSO. At the upper power exchange, the particle swarm optimization algorithm is applied. The procedure of the optimization algorithm is shown in Figure 2.

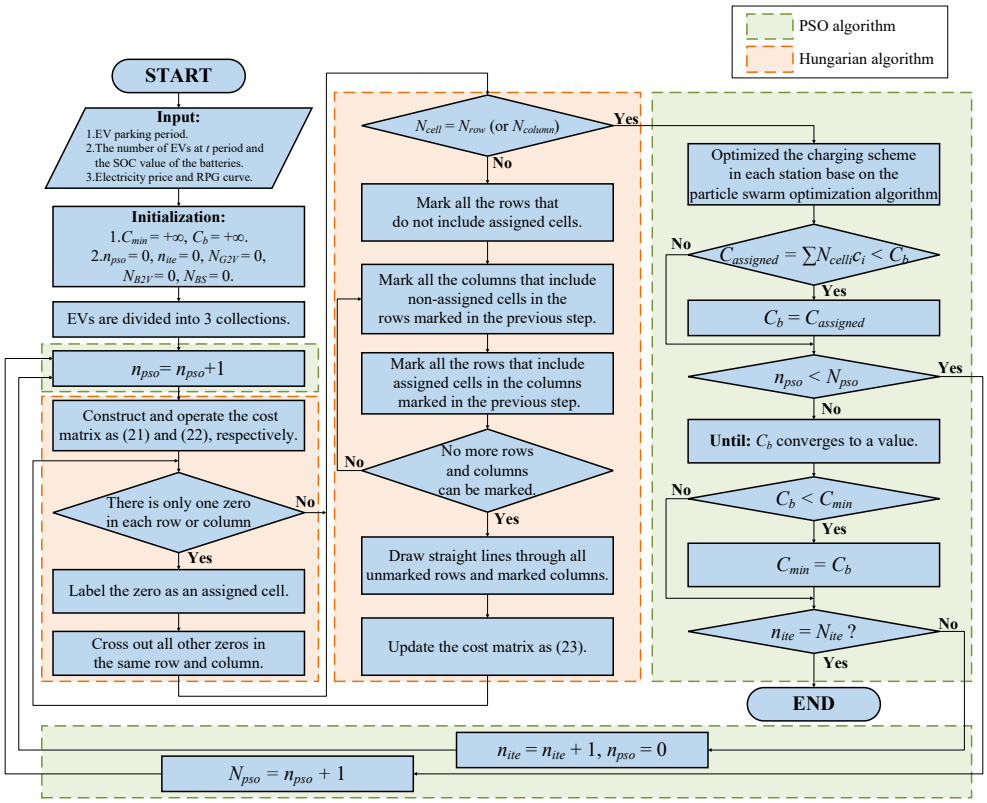

Figure 2. Optimization algorithm procedure.

In Figure 2, the PSO algorithm and Hungarian algorithm are marked using the dashed boxes. The PSO algorithm is represented by a green dashed box, while the Hungarian algorithm is delineated by an orange dashed box. In the Hungarian algorithm box, the calculation procedures are performed for the optimization of EVs' assignment scheme. Equations (21) and (22) ensure there are zero elements existing in each row and column. If there is only one zero in each row or column, the zeros will be named assigned cells and the assignment scheme will be constructed. Otherwise, some calculation procedures are performed to reach the condition.

$$C_{PSO}(t) = \begin{bmatrix} c_{11}(t) & , & c_{12}(t) & \cdots & c_{1(N_b)}(t) \\ c_{21}(t) & , & c_{22}(t) & \cdots & c_{2(N_b)}(t) \\ & & & \vdots & \\ c_{N_b1}(t) & , & c_{N_b2}(t) & \cdots & c_{N_b(N_b)}(t) \end{bmatrix}, \quad (21)$$

$$\begin{cases} c_{ij} = c_{ij} - \min\{c_{i1}, c_{i2}, \cdots, c_{iN_b}\}, i \in [1, 2, \cdots, N_b] \\ c_{ij} = c_{ij} - \min\{c_{1j}, c_{2j}, \cdots, c_{N_bj}\}, j \in [1, 2, \cdots, N_b] \end{cases}, \quad (22)$$

$$\begin{cases} c_{ij} = c_{ij} - \min E_{un} \ , c_{ij} \in E_{un} \\ c\prime_{ij} = c\prime_{ij} + \min E_{un} \ , c\prime_{ij} \in E_{co} \end{cases}, \quad (23)$$

where N_{pso} and N_{ite} are the numbers of particles and iterations in the optimization process, respectively. N_{cell} represents the number of assigned cells. N_{row} and N_{column} represent the row and column number of the matrix, respectively. $C_{\min}$ and C_b are the optimization value at each iteration and in the history data of each particle, respectively, \$. C_{PSO} is the power exchange cost matrix, \$. E_{un} and E_{co} represent the uncovered elements and the elements covered by two lines, respectively. N_{G2V} and N_{B2V} are the number of EVs dispatched to the G2V station and B2V station, respectively.

The cost matrix of EV power exchange is expressed as (21). In the matrix, the number of rows and columns represents that of dispatched EVs and charging stations, respectively. c_{nn} in the element represents the corresponding cost generated by the nth dispatched number of EVs charging in the nth station. In (22) and (23), the calculation procedures of the Hungarian algorithm are described [42].

3. Results and Discussion

3.1. Simulation Parameters

In the simulation process, four power exchange methods and four scenes are employed to verify the effectiveness of the proposed method. The characteristics of the methods and scenarios are shown in Table 1 and Figure 3, respectively.

Table 1. Comparative method characteristics (○: Enable; ×: Disable).

Methods	G2V	B2V	BS	B2B
M1	○	×	×	×
M2	×	○	×	×
M3	×	×	○	×
M4 (proposed method)	○	○	○	○

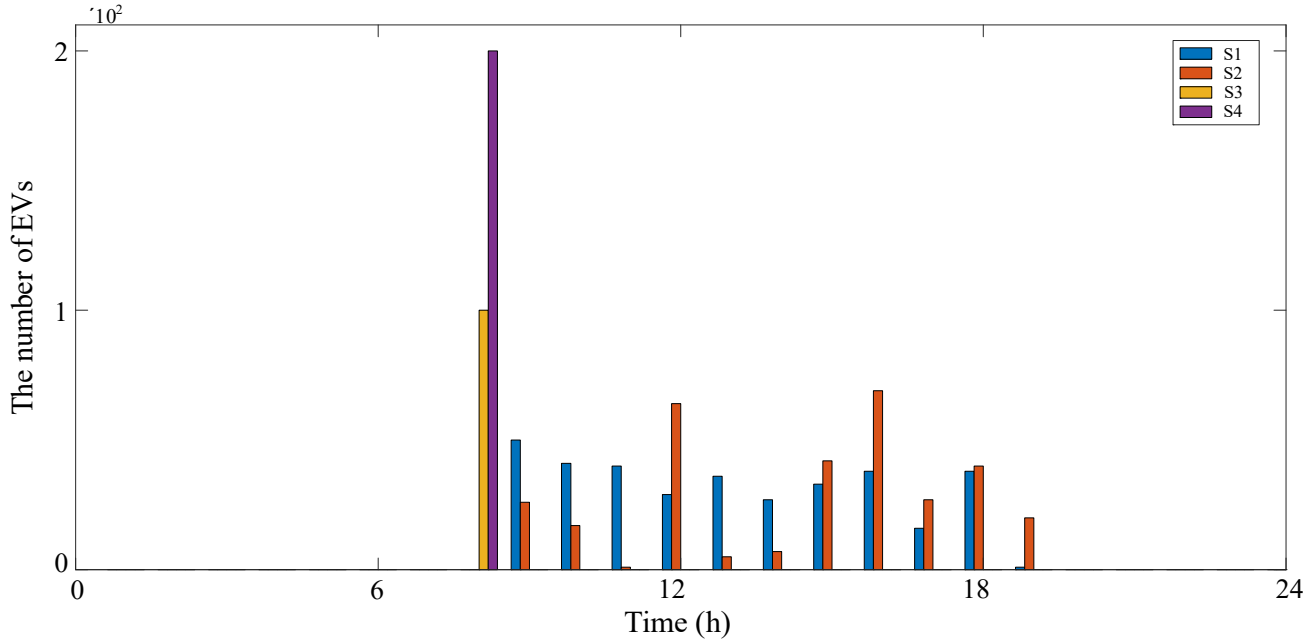

Figure 3. Number of EVs by scenario.

In Table 1, M1, M2, and M3 are the existing EV charging methods, while M4 is the EV charging method proposed in this paper considering the multiple charging modes' coordination. M1 refers to EVs charging solely from the power grid. M2 indicates EVs charge exclusively at B2V stations. M3 indicates the technique that EVs replenish energy in battery swap stations. In M4, multiple charging modes are coordinated.

In Figure 3, the different colors of the bars represent the number of EVs under different scenarios. In S1, the number of EVs is random and the variation laws correspond to the electricity price as shown in (24). Based on S1, the number value is changed from N_{S1} to N_{S2}, and the scenario is named S2. S3 and S4 are utilized to research the influence of EV numbers on the proposed method. So, the number in S3 and S4 is an obvious difference and in the same period. Considering EV users' usage habits, the EV parking time in G2V and B2V stations is set to be 2 h. The object SOC value is considered as the expected SOC value that meets users' driving requirements and is equal to the maximum SOC value.

In the simulation section, the number of EVs is random and fluctuating. EV users' living habits correspond to the electricity price. From the 9th–19th hours, the number of EVs is increased and changes actively according to price. Therefore, t_{s0} and t_{se} are set as 9 and 19, respectively.

$$\begin{cases} n_{S1}(t) = N_{S1} \cdot rand \cdot a_{Grid}(t)\,,\ t_{s0} \le t \le t_{se} \\ n_{S2}(t) = N_{S2} \cdot rand \cdot a_{Grid}(t)\,,\ t_{s0} \le t \le t_{se} \end{cases}, \tag{24}$$

where n_{S1} and n_{S2} are the numbers of EVs supplementing energy in different periods with S1 and S2, respectively. t_{s0} and t_{se} and the starting time and ending time, respectively, h.

The detailed simulation model parameters are from [15,24–26] and presented in Table 2. The SOC value of the EV batteries and the BS station's batteries is set to a single value to simplify the simulation process. Similar to the SOC parameters, the charging power of batteries is also set to a single value.

Table 2. Simulation parameters.

Parameters	Value	Parameters	Value
$SOC_{n,obj}$	0.8	$P_{\max}$ (kW)	70
$SOC_b(t_0)$	0.4	$P_{\min}$ (kW)	0
$SOC_n(t_{ini})$	0.4	$P_{b\max}$ (kW)	70
$SOC_{\max}$	0.8	$P_{b\min}$ (kW)	−7
$SOC_{\min}$	0.2	C_{pur} ($/kWh)	500
$SOC_{b\max}$	0.8	Q_{EV} (kWh)	70
$SOC_{b\min}$	0.2	T (h)	24
γ	2.03	Δt (h)	1
β	5.24×10^{-4}	t_0	1
N_{BS}	140	N_{S1}	50
t_{s0}	9	N_{S2}	100
t_{se}	19		

In Figure 4, the blue bars represent the PV generation and the red line segments indicate the electricity prices of the power grid. It illustrates the electricity price change as well as the photovoltaic generation. The PV generation and the electricity price are floating [10–14]. The real-time electricity price is considered, and the PV generation is assumed to be forecasted accurately. It illustrates the electricity price varies as well as PV generation. The fluctuation in electricity price will affect the power cost of EV charging. The PV generation change will be consumed by charging EVs and influence M2 and M4.

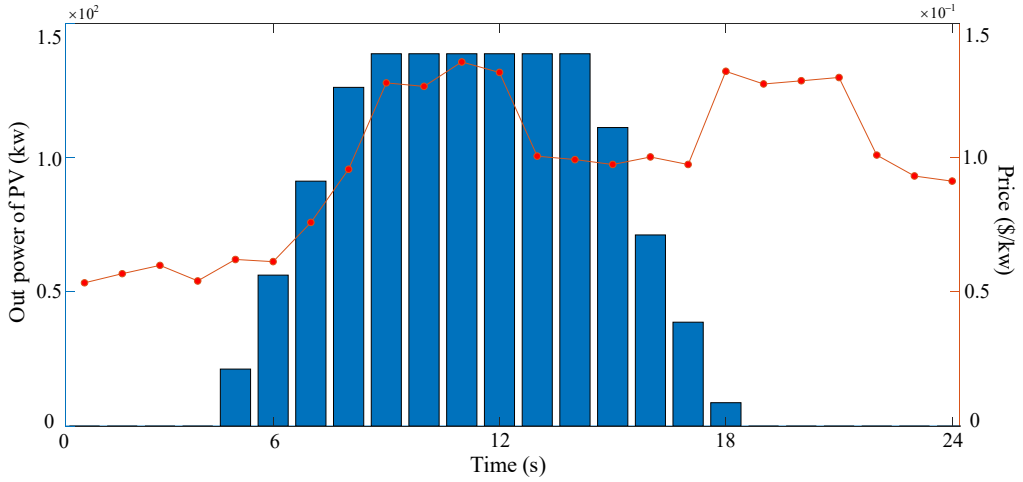

Figure 4. The dynamic parameters in the simulation process.

3.2. Power Exchange Performance Comparison

3.2.1. Algorithm Verification

To verify the advantage of the combination algorithm applied in this paper, a comparison between the PSO algorithm and the combination algorithm is presented in Figure 5. In the PSO algorithm, the number of iterations is set to 50, and the number of particles is set to 100. In Figure 5, the convergence speed of the combination algorithm is significantly faster than that of the PSO algorithm. This is because the optimized EVs' dispatching scheme at each particle is obtained through Hungarian algorithm rearrangement. Therefore, the PSO algorithm's convergence speed is improved.

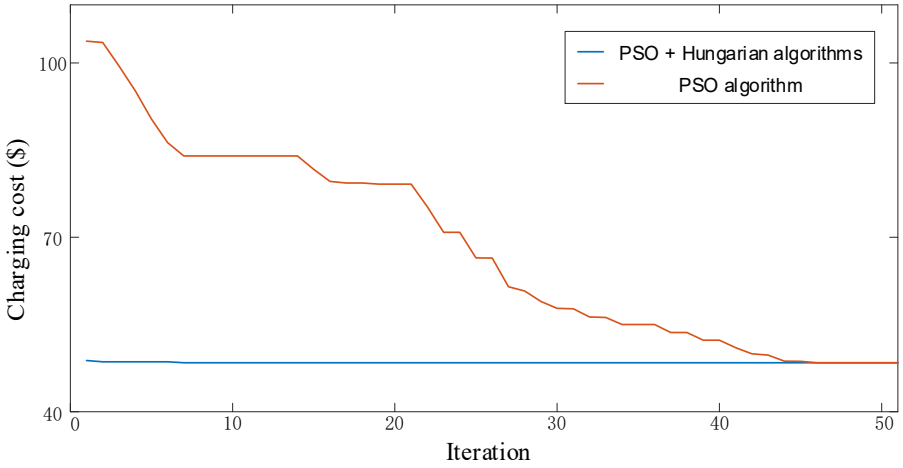

Figure 5. The algorithm comparison with S3.

3.2.2. Method Comparison

In Figure 6, different colored bars are used to represent the costs associated with different methods. The BDC of M1 and M2 are subequal. This is because B2V mode derives from G2V mode and the charging scheme of the two modes is almost equal. The power cost of G2V mode is dependent on the electricity price of the power grid, and that of B2V mode is dependent on the electricity prices of the power grid and PV generation in microgrids. Therefore, the power cost of M2 is less than that of M1 due to the cheap electricity price of PV generation. The BDC of M3 is less than that of M1 and M2 from the 9th–12th hours. This is because the batteries in the BS station charge with a long preparation time and slow charging. EVs have to fast-charge in M1 and M2 due to the limited parking time. From the 13th–16th hours, the BDC of M3 is not too different from that of M1 and M2. This is because there are few batteries with object SOC value, and the batteries in the station

fast-charge to meet the users' driving requirements. Similar to the BDC, the power cost of M3 is less than that of M1 and M2 from the 9th–12th hours because the charging power is concentrated in the period with a low electricity price. From the 12th–14th hours, the power cost of M3 is much more than that of M1 and M2 because of the lower preparation time and fast-charging state in each time interval. From the 9th–11th hours, the BDC and power cost of M4 are equal to those of M3. In the periods, there is only BS mode existing in M4. From the 12th–17th hours, the BDC and power cost of M4 are less than those of M3 due to several modes of coordination. During the 18th hour and 19th hour, the BDC and power costs are more than those of M3 due to the different charging schemes in before periods.

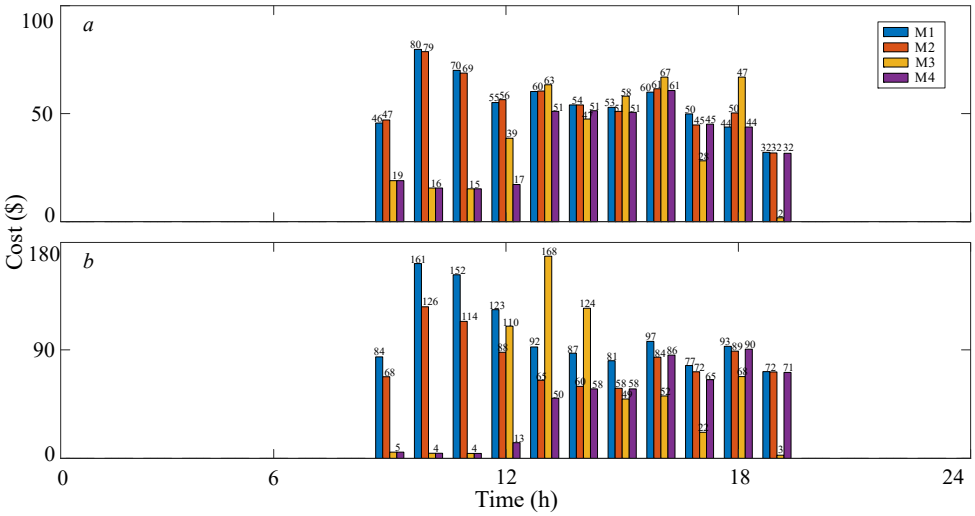

Figure 6. (**a**) BDC and (**b**) power purchasing cost with methods in S1.

The charging power of methods in S1 is shown in Figure 7. The different colored bars are used to distinguish methods, with three shades of green representing the distribution of M4. During the low electricity price periods such as the 1st–7th hours, batteries in the BS station store electricity steadily to reduce the power cost and BDC. From the 9th–13th hours, the charging powers of M1 and M2 are almost equal. However, the power cost of M2 is less than that of M1. This is because the PV generation is consumed locally. In the periods, the charging power of M3 and M4 is less than that of M1 and M2 as the BS station reserves power before. From the 12th–13th hours, the charging power of M4 includes G2V power and B2V power due to the changing electricity price and the PV generation.

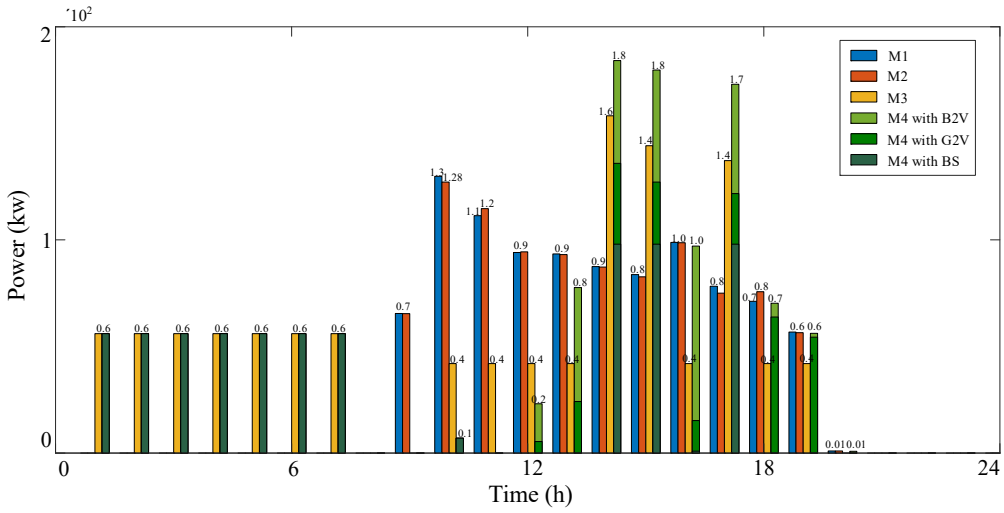

Figure 7. Charging power with methods in S1.

The charging power of M4 is significantly more than that of M3 in most of the periods. However, the cost of M4 is lower than that of M3. This is because the charging modes are coordinated. The PV generation, low electricity price, and slow charging reduce the power cost and BDC. At the 13th hour, B2V and B2B modes are utilized. This is because the PV generation is abundant and the power cost is reduced. In the high electricity price period, B2B mode reduces the power cost. At the 14th hour, the G2V mode is considered in M4 due to low electricity price and abnormal BS operation. From the 14th–19th hours, the charging power of M3 changes due to inadequate reserve power. During this period, several charging modes exist in M4 according to the surplus PV generation and electricity price changes.

In the power exchange, the charging power with modes is optimized, and the optimization object is the minimum cost. Considering the low carbon demand and the low operation cost, the price of EV charging from RPG is assumed to be low. Therefore, RPG is consumed preferentially, and EVs in the B2V station may charge from the power grid when the RPG is consumed completely. From the 13th–17th hours, the RPG is consumed locally. The low-cost operation of BS mode struggles to cover the entire high electricity price period in a day if the number of EVs is too high. Therefore, when the number of batteries with object SOC value in the BS station is insufficient, EVs will be scheduled to different stations to supplement energy in M4.

The costs shown in Table 3 are all in units of $\times 10^3$\$. As shown in Table 3, the total BDC values of M1 and M2 almost have no difference due to similar charging schemes. The total power cost of M2 is less than that of M1 due to the cheaper PV generation. Therefore, compared to G2V mode, B2V mode could locally consume the distributed RPG in the microgrids and reduce the power cost. The BS mode could further reduce the BDC and power cost due to the long preparation time. If the number of EVs supplementing energy is more than the threshold value, the BDC and power cost of the BS mode may be more than those of other modes. At this time, other charging modes should be coordinated to meet users' requirements at a low cost. The BDC and power cost of M4 are less than those of M3. This is because several charging modes are coordinated according to PV generation, electricity price, and swappable batteries. When the swappable batteries are sufficient, EVs are dispatched to the BS station. EVs are dispatched to the B2V station when PV generation is high. B2B mode will be performed in the BS station during the high electricity price period.

Table 3. Cost comparison with S1 ($\times 10^3$\$).

	BDC ($)	**Power Purchasing Cost ($)**	**Total Cost ($)**
M1	0.60	1.13	1.73
M2	0.61	0.90	1.51
M3	0.42	0.61	1.03
M4	0.40	0.51	0.91

In Figure 8, batteries in the BS station charge from the 1st–7th hours. The charging power is dispersed during the low electricity price period. It reduces the charging power in each period and the BDC is decreased. During the high electricity price periods, batteries charge from the other batteries in the BS station to reduce total cost.

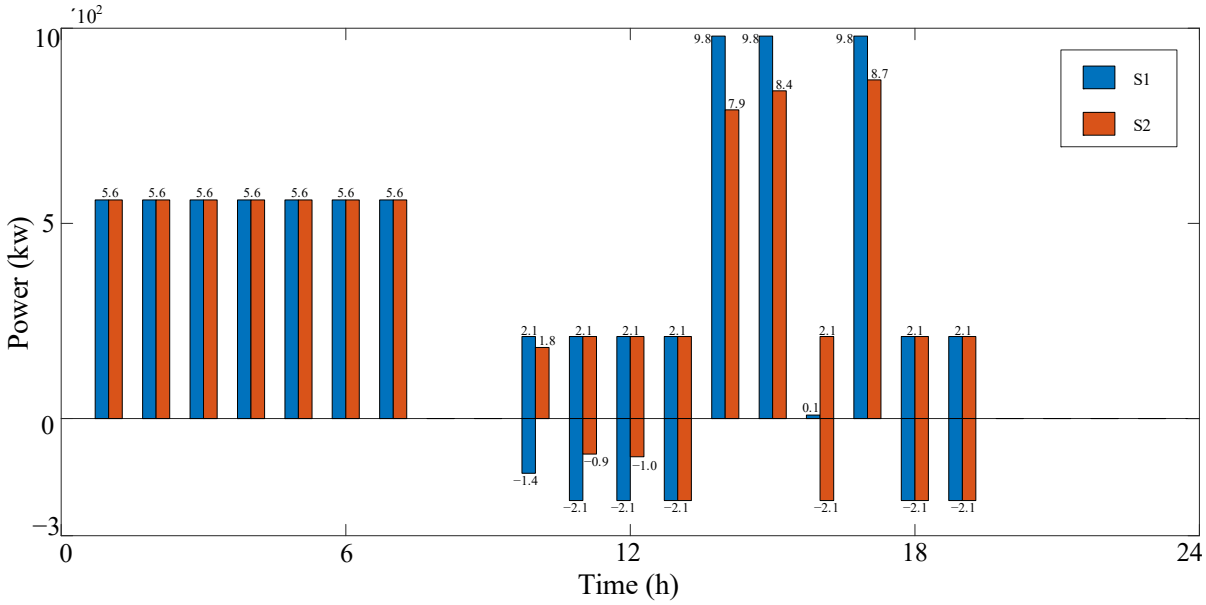

Figure 8. Charging power in BS station with M4.

In Figure 9, the cost of M4 with S1 and S2 changes in each period according to EV number and swappable battery reserve. When the battery reserve is sufficient, the cost of M4 changes slightly such as from the 9th–12th hours in S1 and the 9th–15th hours in S2.

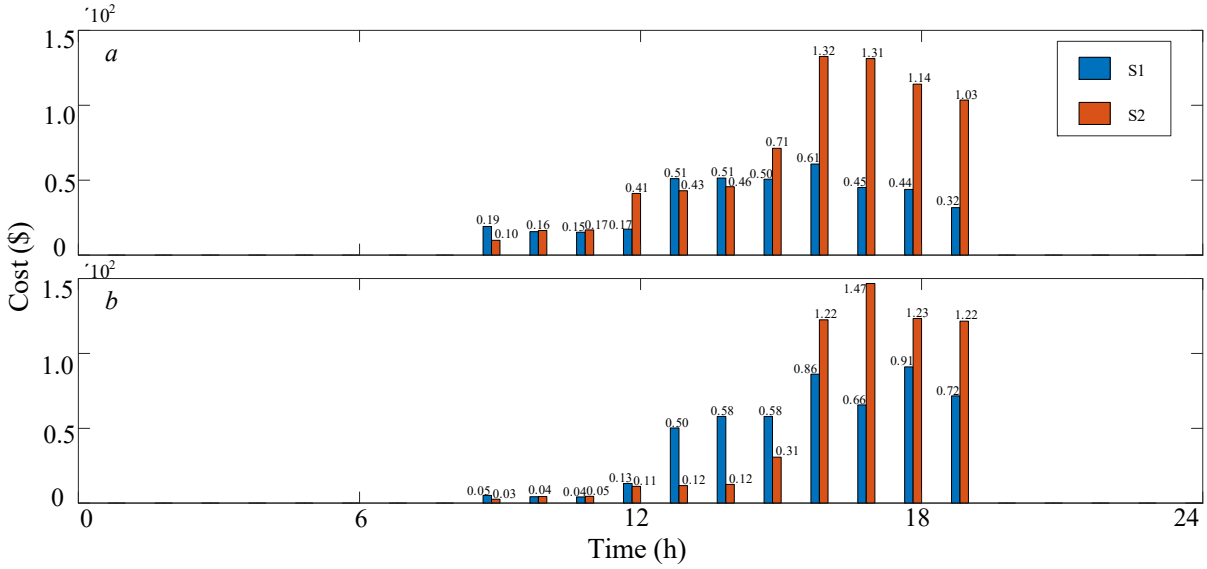

Figure 9. (**a**) BDC and (**b**) power purchasing cost with M4.

In Figure 10, green and yellow bars are used to represent S1 and S2. In Figure 10, from the 1st–7th hours, batteries in the BS station charge from the power grid due to the low electricity price. The low charging power in each period aims to reduce the BDC. When there are enough swappable batteries, EVs are dispatched to the BS station, such as in the 10th hour and 11th hour. Otherwise, EVs are dispatched to other charging stations, such as the periods after the 12th hour.

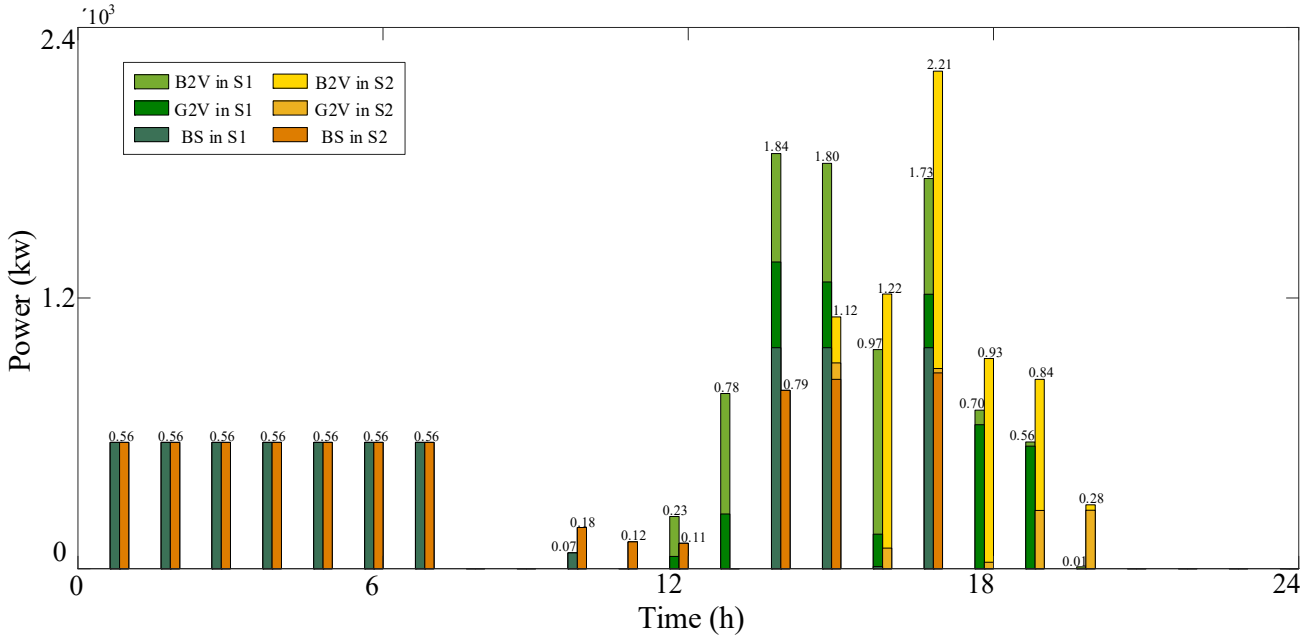

Figure 10. Charging power with M4.

The costs shown in Table 4 are all in units of $\times 10^3$\$. In Table 4, the cost of M4 by scenario is shown. The performance of M4 with S3 and S4 demonstrates that the number of EVs affects the BDC and power cost. The cost is increased slightly when the battery reserve is sufficient.

Table 4. Cost comparison with scenarios ($\times 10^3$\$).

	BDC ($)	Power Purchasing Cost ($)	Total Cost ($)
M4 with S1	0.40	0.51	0.91
M4 with S2	0.73	0.59	1.32
M4 with S3	0.038	0.010	0.048
M4 with S4	0.053	0.015	0.068

3.2.3. EV Number Influence

To further analyze the BS mode, the total charging cost comparison among modes is performed in Figure 11. The charging cost of modes changes with the increasing EV number at the 9th hour in S3. In Figure 11, the cost of G2V mode increases linearly. The cost of B2V mode increases slowly, and the growth rate of B2V mode is equal to that of G2V mode when the EV number reaches a certain value. This is because PV generation is considered in the microgrids and consumed locally by the charging load. Then, the PV generation is consumed completely, and EVs in the B2V station charge from the power grid. The charging cost of BS mode increased slowly due to the sufficient swappable batteries and increased remarkably due to the swappable battery shortage. When the number of EVs is more than the BS station threshold, the batteries in the station have to fast-charge and an exorbitant cost is generated. It can be concluded that the cost of BS charging is cost-effective when the battery reserve is abundant.

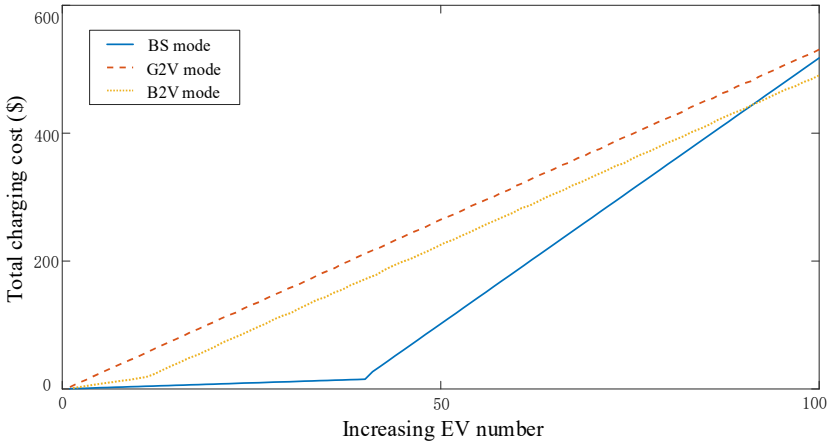

Figure 11. Charging cost changing with the increasing EV number.

4. Conclusions

In this paper, an EV charging method considering multiple charging modes' coordination to meet the various owners' requirements is proposed. EVs are dispatched to the corresponding charging stations according to the charging mode characteristic and the generated cost. In G2V stations, EVs charge from the power grid. In B2V stations, distributed renewable energy generation is considered as the energy provider. In BS stations, the power exchange among batteries and the power grid is considered. The battery energy storage is utilized to reduce the BDC and power cost. In the dispatching process, the PSO algorithm and Hungarian algorithm are applied.

The proposed method ensures that EVs cost-effectively supplement energy. To further improve the users' experience, EVs should be dispatched to charging stations according to the matching between charging mode characteristics and user characteristics. The subject requires additional investigation on how to schedule rational and economic charging schemes in a particular scenario.

Author Contributions: Methodology, funding acquisition, and writing—original draft preparation, L.Z.; validation and supervision, S.-Z.C.; conceptualization, project administration, and writing—review and editing, Z.T.; software and conceptualization, L.T.; project administration and writing—review and editing, T.X. All authors have read and agreed to the published version of the manuscript.

Funding: This research was funded by China Postdoctoral Science Foundation, grant number 2022M720833.

Institutional Review Board Statement: Not applicable.

Informed Consent Statement: Not applicable.

Data Availability Statement: Not applicable.

Conflicts of Interest: The authors declare no conflict of interest.

References

1. Fathi Nassar, Y.; R Aissa, K.; Y Alsadi, S. Air Pollution Sources in Libya. *Res. Rev. J. Ecol. Environ. Sci.* **2017**, *6*, 63–79.
2. Liu, H.; Qi, J.; Wang, J.; Li, P.; Li, C.; Wei, H. EV Dispatch Control for Supplementary Frequency Regulation Considering the Expectation of EV Owners. *IEEE Trans. Smart Grid* **2018**, *9*, 3763–3772. [CrossRef]
3. Ban, M.; Yu, J.; Li, Z.; Guo, D.; Ge, J. Battery Swapping: An Aggressive Approach to Transportation Electrification. *IEEE Electrif. Mag.* **2019**, *7*, 44–54. [CrossRef]
4. Jin, H.; Li, Z.; Sun, H.; Yang, Y.; Wang, B. Coordination on Industrial Load Control and Climate Control in Manufacturing Industry under TOU Prices. *IEEE Trans. Smart Grid* **2019**, *10*, 139–152. [CrossRef]
5. Liu, H.; Huang, K.; Yang, Y.; Wei, H.; Ma, S. Real-Time Vehicle-To-Grid Control for Frequency Regulation with High Frequency Regulating Signal. *Prot. Control Mod. Power Syst.* **2018**, *3*, 13. [CrossRef]
6. Makeen, P.; Ghali, H.A.; Memon, S.; Duan, F. Insightful Electric Vehicle Utility Grid Aggregator Methodology Based on the G2V and V2G Technologies in Egypt. *Sustainability* **2023**, *15*, 1283. [CrossRef]

7. Makeen, P.; Ghali, H.A.; Memon, S.; Duan, F. Smart Techno-Economic Operation of Electric Vehicle Charging Station in Egypt. *Energy* **2023**, *264*, 126151. [CrossRef]
8. Abd El Baset Abd El Halim, A.; Fathi, N.; Bayoumi, E.H.E.; El Khozondar, H.J. Fast Charging of Lithium Ion Battery for Electric Vehicles Applications. In Proceedings of the 8th International Engineering Conference on Renewable Energy & Sustainability (ieCRES 2023), Gaza City, Palestine, 8 May 2023.
9. Lin, Z.; Tang, F.; Yu, C.; Li, H.; Zhong, L.; Wang, X.; Deng, H. Reactive Power Compensation Strategy of the Electric Vehicle Connected to the Distribution Network in the Limit State Considering Voltage Constraint. *Sustainability* **2023**, *15*, 8634. [CrossRef]
10. Chen, Q.; Liu, N.; Hu, C.; Wang, L.; Zhang, J. Autonomous Energy Management Strategy for Solid-State Transformer to Integrate PV-Assisted EV Charging Station Participating in Ancillary Service. *IEEE Trans. Ind. Inform.* **2017**, *13*, 258–269. [CrossRef]
11. Colmenar-Santos, A.; de Palacio-Rodriguez, C.; Rosales-Asensio, E.; Borge-Diez, D. Estimating the Benefits of Vehicle-To-Home in Islands: The Case of the Canary Islands. *Energy* **2017**, *134*, 311–322. [CrossRef]
12. Duan, X.; Hu, Z.; Song, Y. Bidding Strategies in Energy and Reserve Markets for an Aggregator of Multiple EV Fast Charging Stations with Battery Storage. *IEEE Trans. Intell. Transp. Syst.* **2021**, *22*, 471–482. [CrossRef]
13. Knezovic, K.; Martinenas, S.; Andersen, P.B.; Zecchino, A.; Marinelli, M. Enhancing the Role of Electric Vehicles in the Power Grid: Field Validation of Multiple Ancillary Services. *IEEE Trans. Transp. Electrif.* **2017**, *3*, 201–209. [CrossRef]
14. Huang, P.; Lovati, M.; Zhang, X.; Bales, C. A Coordinated Control to Improve Performance for a Building Cluster with Energy Storage, Electric Vehicles, and Energy Sharing Considered. *Appl. Energy* **2020**, *268*, 114983. [CrossRef]
15. Zhou, Y.; Cao, S. Coordinated Multi-Criteria Framework for Cycling Aging-Based Battery Storage Management Strategies for Positive Building–Vehicle System with Renewable Depreciation: Life-Cycle Based Techno-Economic Feasibility Study. *Energy Convers. Manag.* **2020**, *226*, 113473. [CrossRef]
16. Yang, Y.; Jia, Q.-S.; Guan, X.; Zhang, X.Y.; Qiu, Z.; Deconinck, G. Decentralized EV-Based Charging Optimization with Building Integrated Wind Energy. *IEEE Trans. Autom. Sci. Eng.* **2019**, *16*, 1002–1017. [CrossRef]
17. El Khozenadar, H.J.; Albardawil, M.A.; Asfour, M.S.; Abu Khater, I.N.; Fathi, N. DC off Grid PV System to Supply Electricity to 50 Boats at Gaza Seaport. In Proceedings of the 8th International Engineering Conference on Renewable Energy & Sustainability (ieCRES 2023), Gaza City, Palestine, 8 May 2023.
18. Nassar, Y.F.; Alsadi, S.Y.; El-Khozondar, H.J.; Ismail, M.S.; Al-Maghalseh, M.; Khatib, T.; Sa'ed, J.A.; Mushtaha, M.H.; Djerafi, T. Design of an Isolated Renewable Hybrid Energy System: A Case Study. *Mater. Renew. Sustain. Energy* **2022**, *11*, 225–240. [CrossRef]
19. Justin, S.; Saleh, W.; Lashin, M.M.A. Design of Metaheuristic Optimization with Deep-Learning-Assisted Solar-Operated On-Board Smart Charging Station for Mass Transport Passenger Vehicle. *Sustainability* **2023**, *15*, 7845. [CrossRef]
20. Pan, X.; Liu, K.; Wang, J.; Hu, Y.; Zhao, J. Capacity Allocation Method Based on Historical Data-Driven Search Algorithm for Integrated PV and Energy Storage Charging Station. *Sustainability* **2023**, *15*, 5480. [CrossRef]
21. Alsharif, A.; Tan, C.P.; Ayop, R.; Al Smin, A.; Ahmed, A.A.; Kuwil, F.H.; Khaleel, M. Impact of Electric Vehicle on Residential Power Distribution Considering Energy Management Strategy and Stochastic Monte Carlo Algorithm. *Energies* **2023**, *16*, 1358. [CrossRef]
22. Al-Najjar, H.; El-Khozondar, H.J.; Pfeifer, C.; Al Afif, R. Hybrid Grid-Tie Electrification Analysis of Bio-Shared Renewable Energy Systems for Domestic Application. *Sustain. Cities Soc.* **2022**, *77*, 103538. [CrossRef]
23. Buonomano, A. Building to Vehicle to Building Concept: A Comprehensive Parametric and Sensitivity Analysis for Decision Making Aims. *Appl. Energy* **2020**, *261*, 114077. [CrossRef]
24. Barone, G.; Buonomano, A.; Forzano, C.; Giuzio, G.F.; Palombo, A. Increasing Self-Consumption of Renewable Energy through the Building to Vehicle to Building Approach Applied to Multiple Users Connected in a Virtual Micro-Grid. *Renew. Energy* **2020**, *159*, 1165–1176. [CrossRef]
25. Contreras Ocana, J.; Sarker, M.R.; Ortega-Vazquez, M.A. Decentralized Coordination of a Building Manager and an Electric Vehicle Aggregator. *IEEE Trans. Smart Grid* **2018**, *9*, 2625–2637. [CrossRef]
26. Datta, U.; Saiprasad, N.; Kalam, A.; Shi, J.; Zayegh, A. A Price-Regulated Electric Vehicle Charge-Discharge Strategy for G2V, V2H, and V2G. *Int. J. Energy Res.* **2019**, *43*, 1032–1042. [CrossRef]
27. Fu, Y.; Li, Y.Y.; Huang, Y.; Lu, X.; Zou, K.; Chen, C.; Bai, H. Imbalanced Load Regulation Based on Virtual Resistance of a Three-Phase Four-Wire Inverter for EV Vehicle-To-Home Applications. *IEEE Trans. Transp. Electrific.* **2019**, *5*, 162–173. [CrossRef]
28. Zhanga, X.; Peng, L.; Cao, Y.; Liu, S.; Zhou, H.; Huang, L. Towards Holistic Charging Management for Urban Electric Taxi via a Hybrid Deployment of Battery Charging and Swap Stations. *Renew. Energy* **2020**, *155*, 703–716. [CrossRef]
29. Infante, W.; Ma, J.; Han, X.; Liebman, A. Optimal Recourse Strategy for Battery Swapping Stations Considering Electric Vehicle Uncertainty. *IEEE Trans. Intell. Transp. Syst.* **2019**, *21*, 1369–1379. [CrossRef]
30. Choi, D.I.; Lim, D.E. Analysis of the State-Dependent Queueing Model and Its Application to Battery Swapping and Charging Stations. *Sustainability* **2020**, *12*, 2343. [CrossRef]
31. Liu, X.; Zhao, T.; Yao, S.; Soh, C.B.; Wang, P. Distributed Operation Management of Battery Swapping-Charging Systems. *IEEE Trans. Smart Grid* **2019**, *10*, 5320–5333. [CrossRef]
32. Šepetanc, K.; Pandžić, H. A Cluster-Based Operation Model of Aggregated Battery Swapping Stations. *IEEE Trans. Power Syst.* **2020**, *35*, 249–260. [CrossRef]

33. Ahmad, F.; Alam, M.S.; Shariff, S.M. A Cost-Efficient Energy Management System for Battery Swapping Station. *IEEE Syst. J.* **2019**, *13*, 4355–4364. [CrossRef]
34. Wang, Y.; Lai, K.; Chen, F.; Li, Z.; Hu, C. Shadow Price Based Co-Ordination Methods of Microgrids and Battery Swapping Stations. *Appl. Energy* **2019**, *253*, 113510. [CrossRef]
35. Nassar, Y.F.; Abdunnabi, M.J.; Sbeta, M.N.; Hafez, A.A.; Amer, K.A.; Ahmed, A.Y.; Belgasim, B. Dynamic Analysis and Sizing Optimization of a Pumped Hydroelectric Storage-Integrated Hybrid PV/Wind System: A Case Study. *Energy Convers. Manag.* **2021**, *229*, 113744. [CrossRef]
36. Liu, Y.; Yang, J.; Wang, Y.; Chai, Y.; Xu, J. Electric Vehicle Charging and Batteries Swapping Management Strategy with Photovoltaic Generation in Business Districts. *Electr. Power Compon. Syst.* **2019**, *47*, 889–902. [CrossRef]
37. Mahoor, M.; Hosseini, Z.S.; Khodaei, A. Least-Cost Operation of a Battery Swapping Station with Random Customer Requests. *Energy* **2019**, *172*, 913–921. [CrossRef]
38. Yan, J.; Yan, J.; Menghwar, M.; Asghar, E.; Panjwani, M.; Liu, Y. Real-Time Energy Management for a Smart- Community Microgrid with Battery Swapping and Renewables. *Appl. Energy* **2019**, *238*, 180–194. [CrossRef]
39. Clarke, S. *End User Computing Challenges and Technologies: Emerging Tools and Applications*; IGI Global: Hershey, PA, USA, 2007; ISBN 9781599042954.
40. Priya, D.; Ramesh, G. The Hungarian Method for the Assignment Problem, with Generalized Interval Arithmetic and Its Applications. *J. Phys. Conf. Ser.* **2019**, *1377*, 012046. [CrossRef]
41. Cerf, M. Multiple Object Trajectography Using Particle Swarm Optimization Combined to Hungarian Method. *arXiv* **2018**, arXiv:1802.06201.
42. Zeng, L.; Li, C.; Li, Z.; Zhou, B.; Liu, H.; Yang, H. Hierarchical Dispatching Method Based on Hungarian Algorithm for Reducing the Battery Degradation Cost of EVs Participating in Frequency Regulation. *IET Gener. Transmiss. Distrib.* **2020**, *14*, 5617–5625. [CrossRef]